Petr Stodola
Zuzana Jamrichova
Jiri Stodola

ISSN 1333-1124

MODELLING OF EROSION EFFECTS ON COATINGS OF MILITARY VEHICLE COMPONENTS

UDC 25.143

Summary

Military and flying machines (vehicles, aircraft, etc.) operate in extreme conditions and appropriate measures are required to improve the durability of all systems and materials in their subsystems. Protective coatings usually perform this function with great success. Therefore, one of the most pressing needs is the development of high performance coatings for the erosion protection of military machine components (turbines, engines, compressors, turbochargers, intercooler components, etc.). The approach presented in this article is based on the use of computer simulation techniques to model the coating behaviour in simulated erosion conditions. Shear stress and equivalent plastic strain at the coating/substrate interface were used as criteria describing the coating response to particle impact. This article deals with preliminary modelling results in terms of selecting a range of material properties (thickness of internal layers and stress or strain) and the coating structure.

Key words: *wear, erosion, coating, impact, hardness, modelling, military vehicles*

1. Introduction

Erosion of engine compressor blades, for example, is a severe problem for a vehicle operating in desert areas or for aircraft using unpaved landing strips, rough terrain, etc. Damage caused by eroding particles, such as sand, dust or volcanic ash, lowers the engine power, decreases fuel efficiency and, in effect, shortens the engine service life [1]. In extreme cases, extensive erosion damage can lead to engine failure [2]. As a protective measure, complex filtration systems are used to stop eroding particles from entering the engine. Several methods are also employed to improve the erosion resistance of engine compressor components. These methods include thermal processes, e.g. bulk hardening and cryogenic surface treatment, and the use of protective coatings. The latter appears to be the most cost-effective option up to date. In the past, a number of organizations were involved in the development or production of erosion resistant coatings for equipment components. In recent years, however, as the issue of erosion resistance of equipment components became more pressing, we can observe renewed interest in this subject, and, as a result, more companies are becoming engaged. The leading technology in the development of erosion resistant coatings is Physical Vapour Deposition (PVD) with arc, magnetron sputtering and electron beam methods in the forefront. Typically, the PVD coatings, such as nitrides or carbides of transition metals, are much harder than most steels or specialized

alloys and have appreciably lower erosion or wear rates. However, the common challenge is to produce relatively thick coatings to provide prolonged protection before the substrate material is exposed. Generally, as coating thickness increases, residual stress reaches the level where further thickness increase becomes impossible. To address this issue, coating deposition procedures need to be optimised taking into account the residual stress of the coating, as proposed in [3]. As practice shows, harder coatings have improved erosion rate, see Fig. 1.

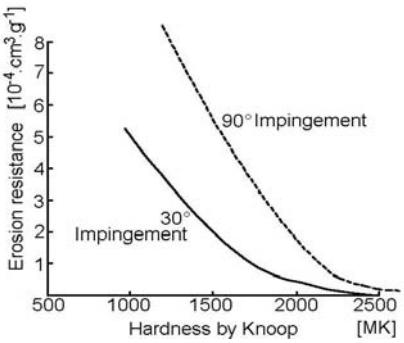

Fig. 1 Erosion resistance (slope of erosion curve) of coating versus hardness

However, very hard coatings are also very brittle and they fail quickly, by fracture and spallation, under repetitive impact load exerted by eroding particles. In erosion test [1], this is evidenced by a relatively short lifetime of the coating despite low erosion rate. Extremely hard coatings do not provide required levels of substrate protection. An obvious solution would be to produce a multi-layer coating combining high hardness and high fracture toughness. In other words, a coating that absorbs most of the impact energy in the top layers and attenuates the stress wave before it reaches the coating/substrate interface. In the approach presented in this article, it was assumed that erosion properties of any erosion resistant coating could be improved by designing multi-layer coatings with internal sub-microstructures consisting of a number of functional layers of different properties. In order to understand how the material responds to the impact load, a computer model simulating the particle impact on hard ceramic coatings was developed. The goal of this research was to develop a basic understanding of the stress and strain distributions within the coating system, with the ultimate objective to develop design principles for new erosion-resistant coatings.

2. Erosion mechanism

Erosion wear is caused by the impact of particles of solids or liquids against the surface of an object. Erosive wear occurs in a wide variety of machinery and typical examples are the damage to gas turbine blades and the wear of impellers. The same as with other mechanisms of wear, mechanical strength does not guarantee wear resistance and a detailed study into material properties is required for wear minimization. Properties of the eroding particle are also significant and are being increasingly recognized as a relevant parameter. The term erosive wear refers to an unspecified number of wear mechanisms which occur when relatively small particles impact on mechanical components. This definition is empirical by nature and relates more to practical considerations than to any fundamental understanding of wear. The known mechanisms of erosive wear are illustrated in Fig. 2 [4]. The angle of impingement is a very important parameter of erosion and it is the angle between the eroded surface and the trajectory of the particles immediately before impact. A low angle of impingement favours wear processes similar to abrasion because the particles tend to track across the worn surface after impact. A high angle of impingement causes wear mechanisms which are typical of erosion. The relationship between wear and the impingement angle of a ductile and brittle material is shown in Fig. 3.

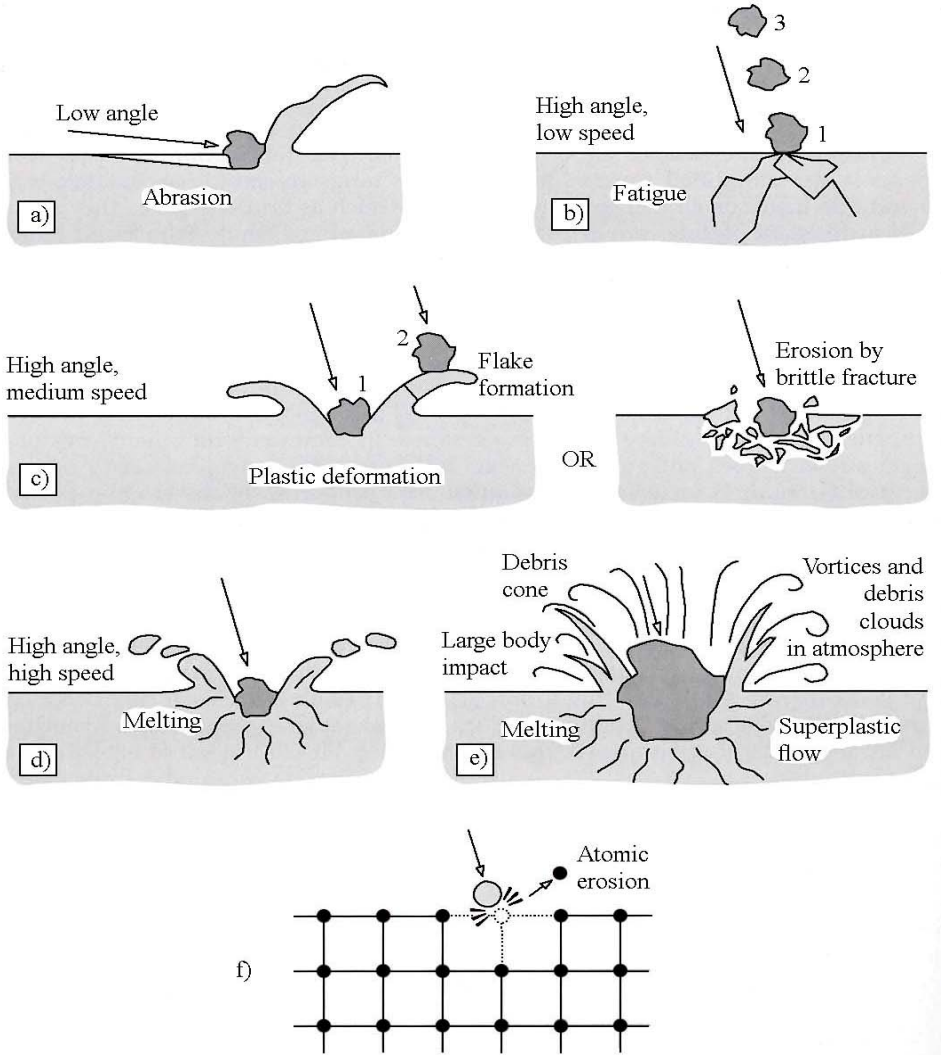

Fig. 2 Mechanisms of erosion: a) abrasion, b) fatigue, c) fracture or plastic deformation, d) melting, e) macroscopic erosion, f) crystal lattice degradation

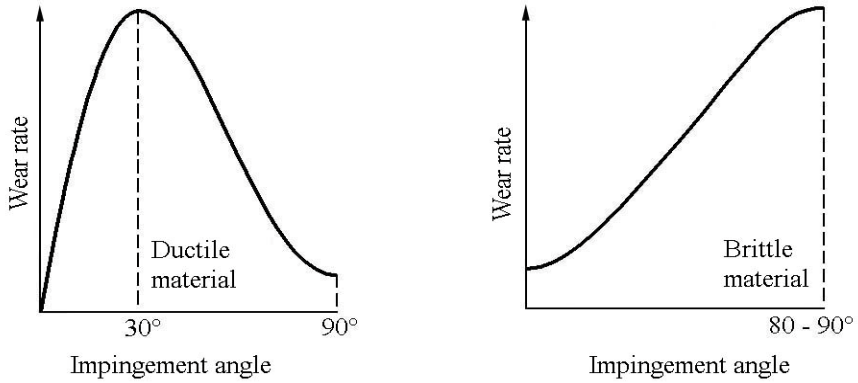

Fig. 3 The effect of impingement angle on wear rates of ductile and brittle materials

The critical part of modelling erosion properties of a material is establishing the primary erosion mechanism. Erosion by solid particle impact is governed mainly by the velocity of eroding particles. An in-depth discussion of impact phenomena in different ranges of particle velocities is given in [5]. In the range of velocities typical of erosion, the dominant mechanisms of erosion of ductile materials (e.g. metals) are plastic fatigue and plastic flow. In the case of brittle materials (e.g. ceramics), brittle fracture and plastic flow are dominant. However, individual

particle impacts do not cause measurable damage to the target (material removal from the target) and the erosion process progresses only as a result of cumulative damage by multiple impacts. Erosion is a complex process, which is affected by many different factors, such as particle size, shape and mass, impact velocity and angle, mechanical properties of target material, and residual stress in the coating. Analysis of coatings consisting of several layers is even more complicated because complex mechanical phenomena at the interfaces between separate layers and their interaction with the substrate have to be analysed. Modelling of the dry erosion process has been attempted by many researches using either the Monte Carlo simulation or single particle models. Many of these models, despite some simplified assumptions, produced results that compared well with experimental results. Hard ceramic coatings, such as TiN, demonstrate a typical brittle behaviour in erosion tests. As discussed in [5], the principal erosion mechanism for brittle coatings is brittle fracture. A more detailed analysis showed that the morphology of fracture is determined by the extent of plastic deformation occurring at the point of contact. In the case of either small velocities or rounded particles (e.g. spherical), the contact is essentially elastic and the resulting fracture is in the form of axially symmetric cone cracks on the periphery of the contact area. When plastic deformation occurs, which is the case with high velocities or angular (sharp) particles, lateral and radial cracks start from the edge of the plastic zone around the indentation area. Under actual erosion conditions and under multiple impacts, many types of cracks are produced, which leads to the material removal when the cracks interlink and propagate to the free surface. When this happens, small flakes of material are removed from the surface. In the case of thin coatings, cracks may reach the interface and cause local delamination and the loss of coating. This also applies to multi-layer coatings. A microscopic examination of erosion scars confirms these mechanisms. From the preceding analysis, it is evident that the erosion properties of the brittle material are defined by the fracture toughness of the material. The cracks appear in material defects and propagate if the stress exerted by the impacting particle $\boldsymbol{\sigma}$ is greater than the critical value $\boldsymbol{\sigma_c}$ for the material. The critical stress for crack propagation is given by the following equation [6]:

$$\sigma_c = \frac{K_C}{\sqrt{\pi \cdot l}}, \tag{1}$$

where

K_C …is the fracture toughness coefficient,

l …is the defect size.

For a TiN coating, a coefficient K_C value of 7 MPam^{-2} and the flow size of 0.1 to 1.0 μm can be assumed. Under these conditions, the critical stress value is between 1.25 and 3.95 GPa. This level of stress (contact pressure) can be produced by a single particle impact [1]. In the case of thin coatings, local delamination under impact occurs when

$$\sigma_c \cdot \sqrt{l} = \frac{K_C(i)}{\sqrt{\pi}}, \tag{2}$$

where

$K_C(i)$ … is the interfacial fractures toughness.

Interfacial fracture toughness is related to interfacial energy [6]. Although it is difficult to quantify this parameter, it is clearly related to the adhesive strength of the coating. The latter is controlled by the coating deposition process and can be easily measured. In summary, a single-layer or a multi-layer erosion resistant coating must perform two major functions:

1. provide a top layer of high hardness and high fracture toughness to delay the onset of cracking and to minimize erosion rate, and

2. prevent high stress waves generated by impacting particles from reaching the coating/substrate interface and thus from causing delamination.

In the conventional approach, many coatings, mostly nitrides or carbides of transition metals, were tried for this moderate success. The main problem was the low fracture toughness of hard coatings. The combination of high hardness and high fracture toughness could not be achieved by monolithic coatings. The obvious solution was multi-layering of hard and ductile phases in order to increase the overall toughness of the coating system. Several systems, such as TiN/Ti, Cr-C/Cr, MO-C/Mo, etc., were investigated both experimentally and by means of the finite element method (FEM) [1], [12], etc. A similar approach was used to optimise wear-resistant coatings. It was demonstrated that multi-layer coatings performed better than their single-layer (monolithic) counterparts although the ductile layer thickness had to be optimised. The second function of the coating is to dissipate the impact energy before it reaches the coating/substrate interface and/or to spread the load as quickly as possible within high modulus top layers. The latter is a potentially useful concept, proposed in [7], to be used in composite structures designed to resist ballistic impact. However, the applicability of the load spreading concept to the erosion resistant coating still has to be investigated. In this paper, coating properties and layering structure were analysed from the point of view of minimising the damage by controlling the parameters, such as shear stresses, that occur at the coating/substrate interface.

3. Energy balance model

Finite element modelling of a coating system under particle impact was performed using ordinary software. To analytically verify numerical calculations, a rudimentary model of a rigid ball impacting an elastic target was developed. It was assumed that the ball impacts on the target at the right angle. An energy balance method was used to solve the model. To calculate the potential energy of elastic deformation of the target, a Hertzian stress distribution in the contact area was assumed. According to the Hertz contact model [8], the force acting on a rigid ball during the static ball indentation is expressed as

$$F = K_0 \cdot E \cdot D^{0,5} \cdot b^{1,5}, \tag{3}$$

where

F is the contact force,
K_0 is the coefficient (0.208),
E is the Young modulus of the target,
D is the diameter of the ball,
b is the indentation depth.

The elastic potential energy E_P of the delamination can be calculated as

$$E_P = \frac{1}{2} K_0 \cdot E \cdot D^{0,5} \cdot b^{2,5}, \tag{4}$$

Subsequently, the kinetic energy of the ball at the time of impact is given by

$$E_K = \frac{1}{2} m \cdot v_0^2, \tag{5}$$

where

m is the mass of the ball,
v_0 is the velocity of the ball at the time of the impact.

In the absence of losses $E_P = E_K$, the maximum indentation of the ball can be calculated as

$$b_{\max} = \sqrt[5]{\frac{m^2 \cdot v_0^4}{K_0^2 \cdot E^2 \cdot D}} . \tag{6}$$

Because equation (4) describes the non-linear relation between the potential energy and the indentation depth, linearization of the load indentation equation was required to calculate the time required for the impacting ball to indent the target. This linearization was done through an assumption that potential energies of the non-linear and linear systems in the indentation range from 0 to $b_{\max}$ should be equal. The linearized expression for elastic potential energy has the following form

$$E_p = E_P^* = \frac{1}{2} k_{eq} \cdot b^2 , \tag{7}$$

where

k_{eq} … is the linear stiffness of the ball or target system.

A comparison of linearized and non-linearized energies $E_P = E_P^*$ produces the expression for the linearized stiffness

$$k_{eq} = K_0 \cdot E \cdot D^{0,5} \cdot b_{\max}^{0,5} . \tag{8}$$

The time required for a ball to fully indent a target may be calculated from equations (5) and (8)

$$t_{imp} = \frac{\pi}{2} \sqrt{\frac{m}{k_{eq}}} \quad . \tag{9}$$

The maximum indentation depth (6) and the time (9) were calculated and compared with the numerical results obtained in the FEM calculations. To check the validity of the model, a set of initial FEM calculations was performed for a rigid ball impacting on a steel substrate with no coating. The displacement of the ball in time was recorded for various substrate properties. An example of the ball displacement in the negative direction of the Y-axis, calculated for the elastic substrate material with no coating and no damping, can be seen in Fig. 4.

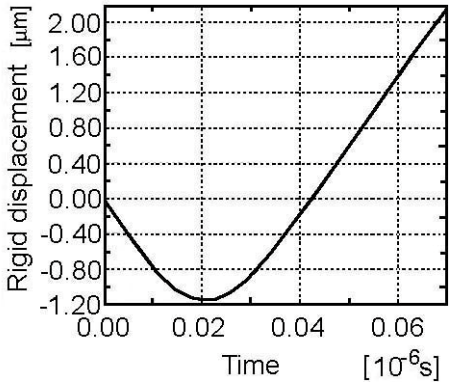

Fig. 4 Results of FEM calculation of rigid ball displacement into a steel target

A steel ball impacting a copper target was modelled using the FEM and the results were compared to the calculation results obtained in [9], and to the experimental results obtained in [1]. The steel ball was modelled as a rigid body of 4.8 mm in diameter, while the copper target was represented by an axisymmetric body of 10 mm in radius and 5 mm in thickness.

The target had elastic-plastic material properties with a constant strain hardening coefficient. Material properties for these calculations are presented in Table 1.

Table 1 Material properties used for the FEM calculation [1]

Property	Fe Ball	Cu Target	Units
Young's modulus	203	138	GPa
Poisson's ratio	0.30	0.30	-
Density	7850	8980	$Kg.m^3$
Yield strength	586	280	MPa
Tangent modulus	260	124.9	MPa

Table 2 Comparison between the FEM calculation of the size of the impact crater and the experimental results

Impact velocity (ms^{-1})	Crater Depth		Difference	Crater Radius		Difference
	FEM (mm)	Experiment (mm)	(%)	FEM (mm)	Experiment (mm)	(%)
54.5	0.2812	0.248	11.8	2.242	2.20	1.9
127.5	0.6792	0.626	7.8	3.299	3.20	3.0
198.7	1.1119	1.058	4.8	4.024	3.87	3.8

Note:

The tangent modulus value is the slope of the elastic region of the stress-strain curve and is also known as the modulus of rigidity or the modulus of elasticity in shear. An example of elastic-plastic behaviour and tangent modulus is given in Fig. 5.

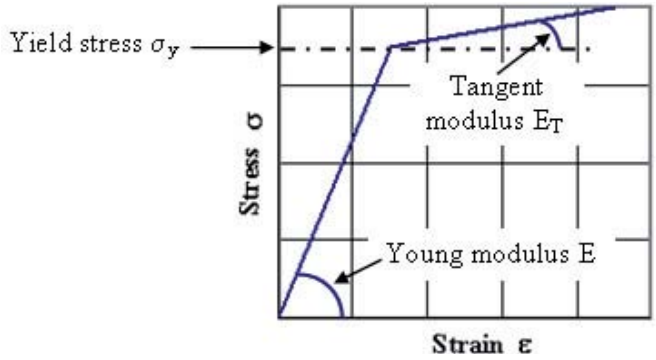

Fig. 5 Elastic-plastic behaviour law

To compare the numerical results with the experimental ones, depths and radii of the crater created in the target material under three different impact velocities were recorded. Table 2 compares the measured and the calculated crater depths and crater diameters for the calculated and the experimentally obtained results. Analysis of these results indicates good agreement between the calculated and the measured results both for the present calculations and those in [9]. The differences between the calculated results can be attributed to different ball material models, the rigid model in the present case vs. the elastic one in [9].

4. Finite element model

For basic understanding of the erosion process in layered systems, a solid mechanics model of a particle impacting on a hard coating deposited on a substrate was developed using FEM, [1], [12], etc. Four types of materials were used in the model: steel, titanium nitride (TiN), titanium (Ti), and aluminium oxide (Al_2O_3). Several FEM models were prepared to perform calculations of the stress and strains at the interface between the substrate and the coating. All models were built using 4-node axisymmetric elements with reduced integration.

A typical FEM with a fine mesh that was used for most calculations is shown in Fig. 6. This model had a radius of 50 μm and it comprised 70 elements. A mesh transition pattern allowed for decreasing the total number of degrees of freedom in the model. Sliding boundary conditions were applied to the nodes along the X and the Y axis. The interaction between the rigid ball and the substrate was modelled using special software [1] in which the contact with no friction between the rigid surface and the deformable body was applied. A constant initial velocity of the ball (77 ms^{-1}) was used in all calculations. The relevant material characteristics were assigned to the appropriate finite elements to create the required coating or the substrate internal structure. The ball radius, mass and velocity were representative of erosion conditions used in the accelerated test performed according to a standard procedure. In all FEMs [10], it was assumed that the considered continuous solid mechanics principles still hold for a range of particle dimensions and coating thicknesses.

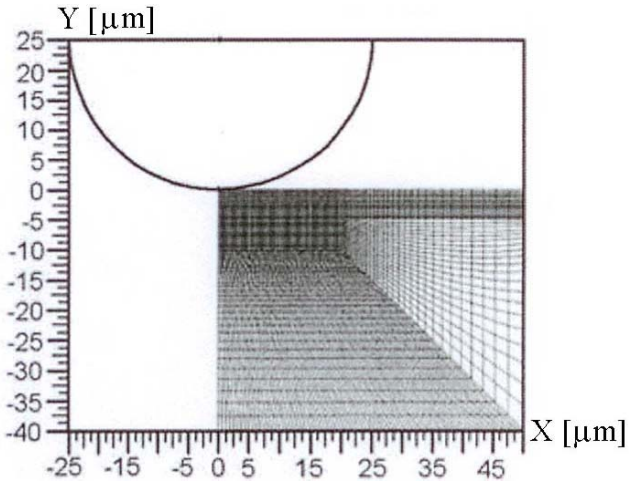

Fig. 6 A typical FEM with a fine mesh

5. Modelling results

A series of calculations were performed for different thickness values of the coating, ranging between 2 and 8 μm, and different values of Young's modulus for the coating, which ranged from 196 to 600 GPa. Equivalent plastic strain in the substrate and the shear stress at the coating/substrate interface were established and analysed. Fig. 7 shows typical distributions in time and space of the equivalent plastic strain and shear stresses as the eroding particle impinges the substrate or the coating system.

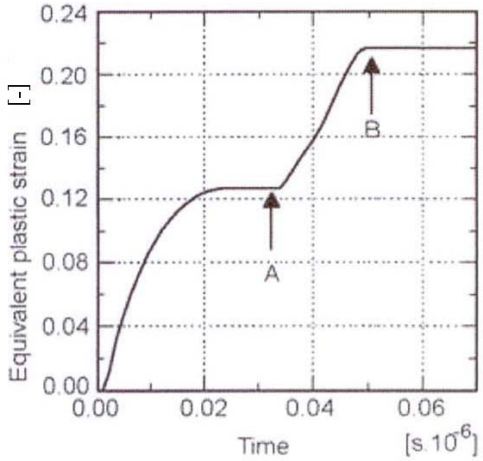

Fig. 7 Development of equivalent plastic strain at the interference in time
(A – particle reverses from the maximum depth, B – particle loses contact with the coating)

Shear Stress (SS) and Equivalent Plastic Strain (EPS) at the coating-substrate interface were used as an evaluation criterion which describes the coating response to a single particle impact. Fig. 8 shows the dependence of these parameters on Young's modulus E_c of the coating. Both parameters were normalized using their respective maximum values obtained for the whole series of calculations.

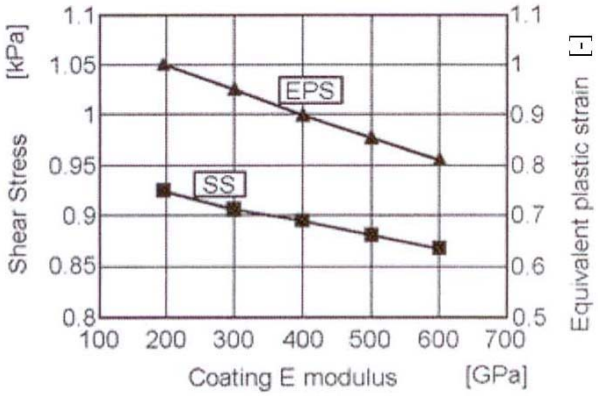

Fig. 8 Shear stress and equivalent plastic strain dependence on Young's modulus of the coating

The greater Young's modulus of the coating, the lower the amount of stress, expressed by shear stress and equivalent plastic strain, that was transmitted to the coating/surface interface. Since a greater Young's modulus usually indicates greater coating hardness, a similar relationship may be expected for coating hardness. In the subsequent numerical test, the previous calculations for shear stress and equivalent plastic strain were repeated with the damping value ($D \neq 0$), i. e. with some level of internal energy loss in the substrate introduced into the computer model. These results are presented in Fig. 9.

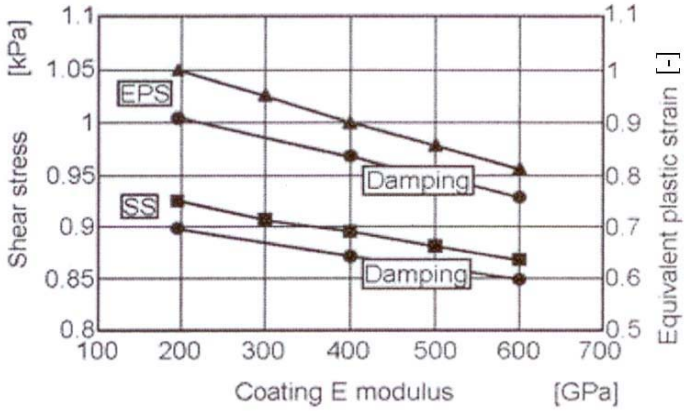

Fig. 9 Effect of damping on shear stress and equivalent plastic strain

As shown in this figure, damping lowered the equivalent plastic strain magnitude by approximately 10 %. The damping effect on shear appeared to be smaller by approximately 3 %, but still noteworthy. On the other hand, damping did not change the calculation results qualitatively. Therefore, since calculation times for the cases with damping were much longer, at this stage of model development, damping was not taken further into account. Another characteristic investigated with this model was the effect of the coating thickness. Fig. 10 shows the shear stress and equivalent plastic strain dependences for coatings ranging in thickness from 2 to 8 μm. The shear stress showed a gradual decrease as the coating thickness increased. This correlation may be expected as simple common sense suggests that a thicker coating would be more effective in providing physical separation between the substrate and the surface of the coating where the impact occurs.

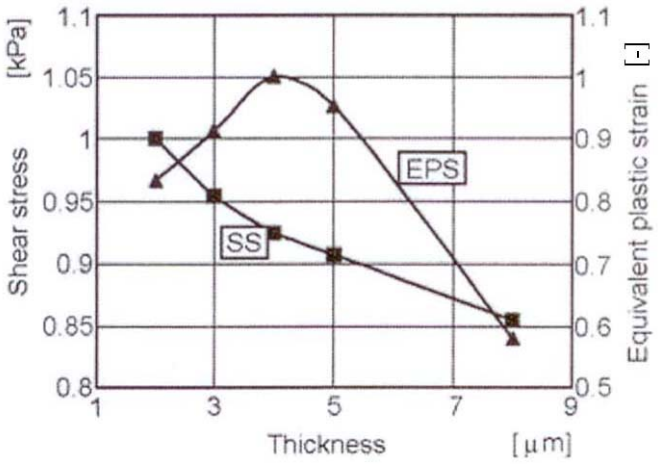

Fig. 10 Effect of coating thickness on shear stress and equivalent plastic strain magnitude at the coating/surface interface

In simplified analyses, one can assume that, for a given coating material, stress wave speed is proportional to the coating modulus. Then, in the absence of internal losses, the results can be interpreted as results of a load spreading within high modulus coatings. The higher modulus of thickness of the coating, the more effective load spreading was observed. With the exception of the results in Fig. 10, equivalent plastic strain characteristics showed a similar trend as those for shear stress. However, the equivalent plastic strain curve demonstrated the presence of a local maximum for the 4 μm thick coating. This result can be explained by analysing the equivalent plastic strain distribution in a radial direction of the model. The equivalent plastic strain distribution versus the true radial distance is shown in Fig. 11. It is evident that for relatively thick coatings, the distribution of equivalent plastic strain is bell-shaped. When the coating becomes thinner, the maximum of equivalent plastic strain curve moves off centre, creating a ring of equivalent plastic strain values around the impact centre. This phenomenon is actually observed in experiments. In the case of brittle materials, the edge of the small plastic zone around the impact area is a starting point for radial or lateral cracks. In all cases presented in Fig. 11, greater Young's modulus resulted in lower stress at the coating/substrate interface, similar to the results presented in Figs 9 and 10. It means that harder coatings are more resistant to plastic deformation, which again confirms the validity of the computer model. From the preceding discussion and data presented in Figs 10 and 11, it appears that the shear stress at the coating interface can be effectively used as a single criterion to evaluate coating response to the impact load. Interpretation of equivalent plastic strain data is more difficult since not only the maximum value has to be considered but also the radial distribution. Fig. 12 shows the shear stress dependence on Young's modulus and the coating thickness. Greater Young's modulus and increased coating thickness resulted in lower stress at the coating/substrate interface. However, increasing the coating hardness and thickness has its practical limits, one of them being the residual stress build-up during deposition. Besides, in gas turbine applications, the coating thickness is limited in order not to affect the aerodynamic properties of the blades. Therefore, higher coating performance has to be achieved by the multi-layering of hard and ductile phases in order to increase the overall toughness of the coating system.

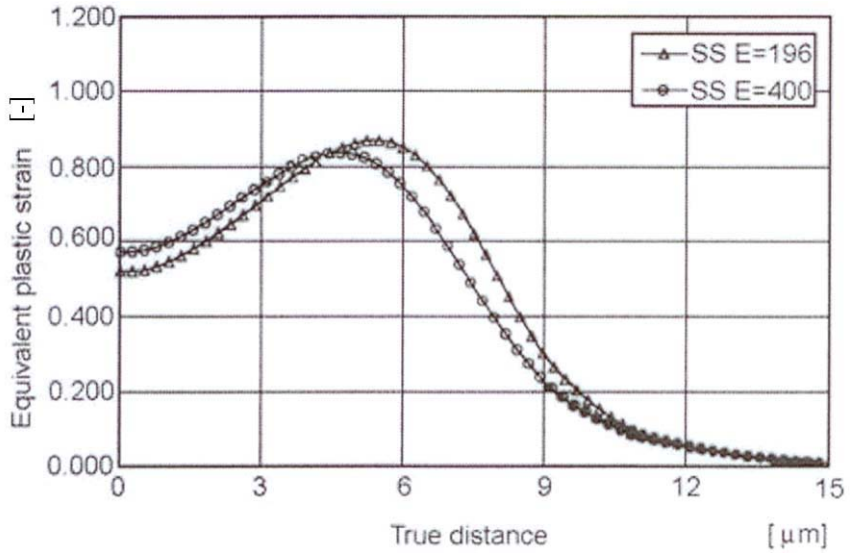

Fig. 11 Equivalent plastic strain distribution in radial direction

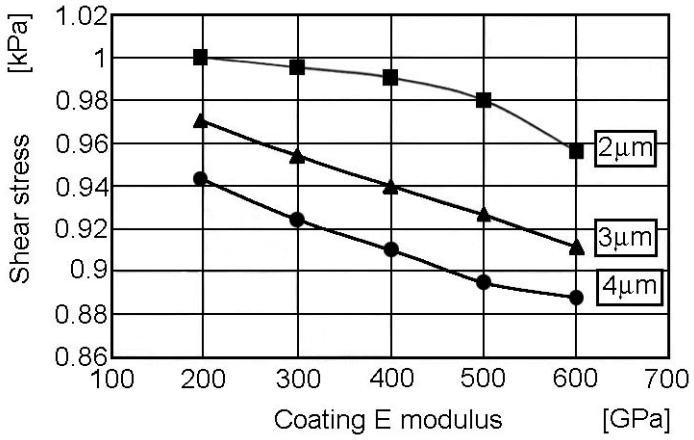

Fig. 12 Shear stress dependence on the Young modulus and the thickness of the coating

6. Conclusion

The modelling results presented in this article may be considered as an extended verification of the computer model rather than a set of coating design principles. However, good qualitative agreement with the known experimental results and observations was obtained. Harder and thicker coatings were found to be more effective in lowering the stress level at the coating/substrate interface. Additionally, coatings benefited from the presence of a soft bond layer that contributed to the lowering of stresses at the interface and possibly to the increase in effective fracture toughness of the coating. In quantitative calculations, internal energy losses in the substrate material need to be included. The preliminary modelling results indicate that, in the absence of internal losses, a lower magnitude of stresses at the coating/substrate interface can be attributed to the load spreading effect of the high modulus coating materials. The further part of research will be verified experimentally by producing trial coatings and evaluating them through microstructural and functional tests.

Acknowledgement

This paper was elaborated with the support of the NATO RTA AVT 109 team and partially sponsored by the Ministry of Defence of the Czech Republic within the framework of Research Establishment Development Project.

REFERENCES

[1] Bielavski,M.–Beres,W.–Patnaik,C.P. Modelling of a Single–Particle Impact Response of Erosion–Resistant Coating. RTO–AVT–109. Paper Nr. 23–1–15, 2004

[2] Paramesvaran,R.V et al. Erosion resistant Coatings for Compressor applications. Advances in High Temperature Structural Materials and Protective Coatings, 1994. Editor Koul, K. A. NRC Canada

[3] Bielawski, E.F et al. The Effect of Process Parameters on the Mechanical and Microstructural Properties of Thick TiN Coatings. Proceedings of the SVC Dallas, 2004

[4] Stachowiak,W.G.–Batchelor,W.A. Engineering Tribology. Third Edition. Elsevier Inc., 2005. ISBN 978-0-7506-7836-0 (801 p)

[5] Hutchings,M.I.–Field,E.J. Surface Response to Impact. Materials at High Strain Rates. Editor T. Z, Blazynski: Elsevier Ltd., 1987

[6] Ohring,M. The Material Science of Thin Films. Academic Press, 1992

[7] Gupta,M.Y.–Ding,L.J. Impact Load Spreading in Layered Materials and Structures: Concept and Quantitative Measure. In: International Journal of Impact Engineering. Vol. 27, 2002

[8] Joung,C.W. Remark's Formulas for Stress and Strain. McGraw-Hill, 1989

[9] Woytowitz,J.P.–Richman,H.R. Modelling of Damage from Multiple Impacts by Spherical Particles. Wear, Vol. 233 – 235, 1999

[10] Stodola,J. Advances in Special Technique. Monograph, 1st Edition. Brno: UoD, 2010. p 202. ISBN 978-80-7231-716-5

[11] Stodola,J. Modelling of Ball Impacts on Coatings and Erosion of Special Technique Components. Advances in Military Technology. Vol. 6, No 2, Brno, 2011. ISSN 1802-2308

[12] Peyraut,F,–Seichepine,J.-L.–Coddet,C.–Hertter,M. Finite Element Modelling of Abradable Materials – Identification of Plastic Parameters and Issues on Minimum Hardness Against Coating's Thickness. Int. J. Simul. Multidisci. Des. Optim. **2**, 209–215 (2008)

Submitted: 14.5.2012

Accepted: 13.9.2012

Doc. dr. Petr Stodola
University of Defence Brno
Faculty of Economics and Management
Kounicova Str. 65
662 10 Brno, Czech Republic

Doc. dr. Zuzana Jamrichova
Alexander Dubcek University of Trencin
Faculty of Special Technology
Studentska Str. 1
911 50 Trencin, Slovak Republic

Prof. dr. sc. Jiri Stodola
University of Defence Brno
Faculty of Military Technology
Kounicova Str. 65
662 10 Brno, Czech Republic